

Absolute $^{13}\text{C}/^{12}\text{C}$ Isotope Amount Ratio for Vienna Pee Dee

Belemnite from Infrared Absorption Spectroscopy

Adam J. Fleisher^{1,4,✉}, Hongming Yi^{1,4,5}, Abneesh Srivastava¹, Oleg L. Polyansky^{2,3}, Nikolai F.

Zobov³, and Joseph T. Hodges¹

¹Material Measurement Laboratory, National Institute of Standards and Technology,
Gaithersburg, MD, USA

²Department of Physics and Astronomy, University College London, London, UK

³Institute of Applied Physics, Russian Academy of Sciences, Nizhny Novgorod, Russia

⁴These authors contributed equally: Adam J. Fleisher, Hongming Yi

⁵Present affiliation: The Department of Civil and Environmental Engineering, Princeton
University, Princeton, NJ, USA

✉To whom correspondence should be addressed:

e-mail: adam.fleisher@nist.gov

phone: 301-975-4864

mailing address: National Institute of Standards and Technology, 100 Bureau Drive,

Mailstop 8320, Gaithersburg, MD 20899, USA

Measurements of isotope ratios are predominantly referenced to physical artifacts. Among them are the reference materials (RMs) used to realize the Vienna Pee Dee Belemnite (VPDB) scale for stable carbon isotope analysis¹—RMs which remain traceable to the original Pee Dee Belemnite artifact furnished by Lowenstam and Urey². However, these RMs have proven unstable or depleted over time³—mirroring issues that led to a revised International System of Units (SI)⁴. A campaign to elucidate the stable carbon isotope ratio of VPDB, $R(^{13}\text{C}/^{12}\text{C})_{\text{VPDB}}$, is underway⁵, but independent measurement techniques are desired. Here we report an accurate value for $R(^{13}\text{C}/^{12}\text{C})_{\text{VPDB}}$ inferred from infrared absorption spectroscopy—fulfilling the promise of this fundamentally accurate approach⁶. Our results agree with the recently recommended $R(^{13}\text{C}/^{12}\text{C})_{\text{VPDB}}$ value derived from mass spectrometry⁵, and therefore advance the prospects of SI-traceable isotope analysis. Further, our calibration-free method could improve mass balance calculations and enhance isotopic tracer studies in CO₂ source apportionment.

Small variations in the isotopic abundances of common nuclei such as carbon, oxygen and hydrogen occur naturally. The isotope-delta notation is a useful expression for precision stable isotope analysis and is generally defined as $\delta^i\text{E} = R(^i\text{E}/^j\text{E})_{\text{sample}}/R(^i\text{E}/^j\text{E})_{\text{ref}} - 1$, where i is the heavier isotope mass number of element E (e.g., ¹³C), j is the lighter isotope mass number of E (e.g., ¹²C), and $R(^i\text{E}/^j\text{E})_{\text{sample}}$ and $R(^i\text{E}/^j\text{E})_{\text{ref}}$ are the absolute isotope ratios of an unknown sample and a reference material, respectively (e.g., $R(^{13}\text{C}/^{12}\text{C})_{\text{sample}}$ and $R(^{13}\text{C}/^{12}\text{C})_{\text{ref}}$)⁷. The δ notation—expressed *per mille* using the symbol ‰, where $1\text{‰} \equiv 1 \times 10^{-3}$ —allows for the convenient expression of exceedingly small differences in isotope composition, and thus an accessible discussion of subjects as diverse as variability in atmospheric composition, climatology, geochemistry, ecology, and dietary evolution and networking.

To measure small differences on a δ scale, ultraprecise analytical techniques such as isotope ratio mass spectrometry (IRMS)⁸ and Fourier transform infrared spectroscopy⁹, based on the identical treatment of sample and reference, are commonly used. Although δ values can be determined with a precision of ≤ 0.01 ‰, absolute isotope ratio measurements of $R(^iE/^jE)_{\text{sample}}$ with commensurate accuracy have not been possible because of either systematic uncertainties in the values of $R(^iE/^jE)_{\text{ref}}$ or the achievable uncertainty in primary methods such as calibration using synthetic isotope mixtures. For example, the most recent evaluation of the VPDB reference ratio that underpins the $\delta^{13}\text{C}$ scale, $R(^{13}\text{C}/^{12}\text{C})_{\text{VPDB}}$, reported uncertainties that were more than 100-fold greater than the achievable precision⁵. The lack of independent experimental techniques for stable carbon isotope ratio measurements has generally impeded the assessment of uncertainty in $R(^{13}\text{C}/^{12}\text{C})_{\text{ref}}$ values and confounded efforts to correct for their respective drifts over time³.

The δ notation has additional limits. For example, δ values are approximately a linear function of mole fraction only for very small differences between $R(^iE/^jE)_{\text{sample}}$ and $R(^iE/^jE)_{\text{ref}}$, and multiple RMs are required to establish linearity¹. For samples with large differences between $R(^iE/^jE)_{\text{sample}}$ and $R(^iE/^jE)_{\text{ref}}$ (e.g., samples enriched or depleted in ^{13}C , or extraterrestrial samples), δ values are a highly nonlinear function of mole fraction⁷, and precision is generally degraded when measuring sample values far from the scale definition ($\delta^iE = 0$). For several applications, direct measurements of $R(^iE/^jE)_{\text{sample}}$ or atom (mole) fraction would be advantageous. These include tracer studies for enriched compound- or position-specific isotope analysis¹⁰ and the calculation of mixing ratios in complex systems using a mass balance equation (e.g., systems with two or more sources and/or sinks of variable isotopic composition⁷). From a standards and

metrology perspective, direct measurements of $R(^iE/^jE)_{\text{sample}}$ would enable detailed studies of drifts in primary RMs³ and SI traceable isotope ratio determinations⁵. Accurate measurements of $R(^iE/^jE)_{\text{sample}}$ that are traceable to intrinsic physical invariants would also maintain compatibility with historical δ notation scales by underpinning the isotope ratios of the primary and secondary RMs. This is highly desirable, given that the ratio-of-ratios approach conveniently expressed by the δ notation is inherently susceptible to temporal instability and physical inhomogeneity in the required chain of RMs and two-point calibration schemes. Finally, reliable scales that eliminate RMs altogether are desirable when measuring isotope ratios in extreme environments like those encountered during solar system exploration. There, carrying bulky and consumable RMs can be cost-prohibitive and pre-launch calibration routines are necessary to validate measurements like the isotopic composition of the modern Martian atmosphere¹¹.

Optical methods to measure $R(^iE/^jE)_{\text{sample}}$ directly—circumventing the δ notation—have been proposed for decades⁶. Several notable efforts were focused on improving measurement precision and studied infrared transitions over a narrow wavelength range¹²⁻¹⁵. That approach is problematic even when the absorption cross-sections—intrinsic molecular quantities which scale the isotope amounts—are well known¹⁶. Transitions involving different isotopic substitutions of the same molecule that occur at wavelengths near to one another often originate from very different rotational states, and consequently substantial temperature biases are introduced. Those biases can be mitigated through a high degree of temperature control^{17,18}, or by studying pairs of transitions with nearly identical lower-state rotational energy¹⁹. While these prior proposals and proof-of-principle demonstrations collectively suggest that accurate optical measurements of $R(^iE/^jE)_{\text{sample}}$ may be possible without calibrations, each prior work was limited

by either the aforementioned temperature biases or by uncertainties in the chosen absorption cross-sections. As a result, the absolute isotope ratios of RMs inferred from accurate infrared absorption spectroscopy measurements have never been compared with SI-traceable mass spectrometry values.

Here we overcome both experimental hurdles using accurately known absorption cross-sections for carbon dioxide (CO₂) transitions from two distinct wavelength regions—effectively eliminating temperature biases. The results are the first measurements of $R(^iE/^jE)_{\text{sample}}$ by direct absorption spectroscopy with an uncertainty commensurate with calibrated mass spectrometry. By also performing state-of-the-art IRMS on our CO₂-in-air gas samples, we infer $R(^{13}\text{C}/^{12}\text{C})_{\text{VPDB}} = 0.011125 \pm 0.000043$. The value of $R(^{13}\text{C}/^{12}\text{C})_{\text{VPDB}}$ derived from our unified measurement approach is in excellent agreement with other recently reported values⁵ and differs significantly from the historic value of Craig²⁰. Consequently, our results demonstrate the potential for perpetual and direct SI-traceability in stable carbon isotope analysis, thus circumventing limitations associated with curation and further propagation of the new physical artifact standards that underpin the $\delta^{13}\text{C}$ VPDB scale²¹.

Our accurate isotope ratio infrared spectroscopy (AIR-IS) instrument, illustrated in Fig. 1A, is a robust platform measuring the mole fraction of both ¹³CO₂ and ¹²CO₂, and therefore the stable carbon isotope ratio of a gas sample. Typical relative measurement precision of $R(^{13}\text{C}/^{12}\text{C})_{\text{sample}}$ for a 3 min spectral acquisition was 0.2×10^{-3} , with a best recorded relative precision of 0.13×10^{-3} [comparable to the World Meteorological Organization / International Atomic Energy Agency (WMO/IAEA) extended compatibility goal for $\delta^{13}\text{C}$ of $\pm 0.1 \text{‰}$ ²²]. We simultaneously probed ¹³CO₂ and ¹²CO₂ rotational-vibrational transition pairs with nearly

identical lower-state quantum numbers and lower-state energies, and therefore effectively identical Boltzmann population factors (Supplementary Information, Sections S1 and S3). Using diode lasers centered near wavelengths of 2.0 μm ($^{13}\text{CO}_2$) and 1.6 μm ($^{12}\text{CO}_2$) and high-reflectivity mirrors to form a single sample cell, the AIR-IS instrument created overlapping intra-cavity mode volumes for both wavelengths. This arrangement, combined with synchronous acquisition of the spectra, largely eliminated the influence of spatial-temporal temperature and pressure variations on the measured peak area ratios.

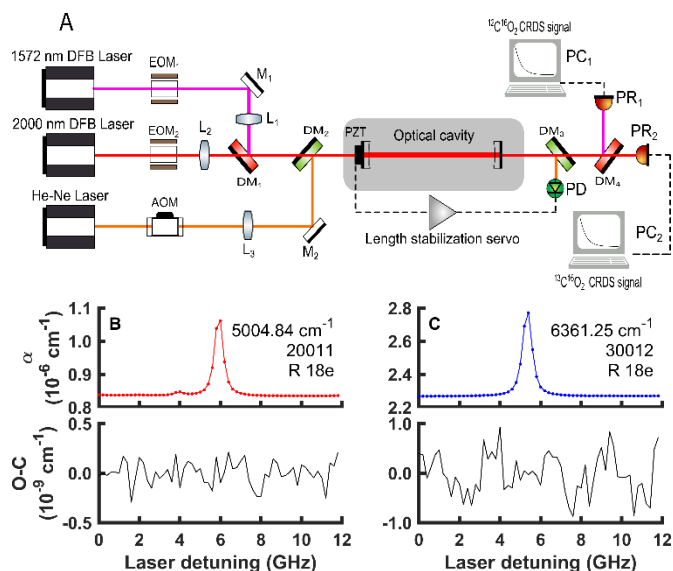


Fig. 1. Accurate isotope ratio infrared spectroscopy (AIR-IS). **A.** The spectrometer synchronously interrogated two infrared transitions using diode lasers at wavelengths nominally equal to 2.0 μm ($^{13}\text{C}^{16}\text{O}_2$) and 1.6 μm ($^{12}\text{C}^{16}\text{O}_2$), respectively. Frequency agile, rapid-scanning was accomplished via two electro-optic modulators (EOM) driven by individual radiofrequency function generators. The length-stabilized optical enhancement cavity and sample cell provided effective path lengths of 12 km and 4.5 km at 2.0 μm and 1.6 μm , respectively. Laser light transmitted by the cavity was split at a dichroic mirror (DM) and then directed onto one of the two photoreceivers (PR). Additional abbreviations: AOM, acousto-optic modulator; M, reflective mirror; L, lens; PD, photodetector; PC, personal computer. **B-C.** Representative high-resolution cavity ring-down absorption spectra of $^{13}\text{C}^{16}\text{O}_2$ and $^{12}\text{C}^{16}\text{O}_2$ for a sample of NIST Standard Reference Material 1720 Northern Continental Air ($\chi_{\text{CO}_2} = 393.23 \mu\text{mol/mol}$; $\delta^{13}\text{C} = -8.6 \text{‰}$).

The absorption spectra of $^{13}\text{C}^{16}\text{O}_2$ and $^{12}\text{C}^{16}\text{O}_2$ in air at mole fractions within the range of natural terrestrial and marine abundances are shown in Fig. 1B-C. These spectra were measured using cavity ring-down spectroscopy and correspond to a reference sample of North American continental air with a value of $\delta^{13}\text{C} = -8.6 \text{ ‰}$ realized by the WMO Global Atmosphere Watch Central Calibration Laboratory at the National Oceanic and Atmospheric Administration (NOAA). We report similar peak absorption coefficients for both isotopologues, and thus similarly precise fits of the individual mole fractions $\chi = \frac{k_B T}{c S(T) p} \int \alpha(\nu) d\nu$, where c is the speed of light in a vacuum, k_B is the Boltzmann constant, T is the sample temperature, p is the total sample pressure, $S(T)$ is the unweighted temperature-dependent transition intensity (i.e., not weighted by natural terrestrial isotopic relative abundances), and $\alpha(\nu)$ is the measured absorption coefficient as a function of frequency ν . Assuming that all stable isotopes of C (^{13}C , ^{12}C) and O (^{18}O , ^{17}O , ^{16}O) are randomly distributed amongst the corresponding isotopologues of CO_2 , then $R(^{13}\text{C}/^{12}\text{C})_{\text{sample}} = \chi(^{13}\text{C}^{16}\text{O}_2)/\chi(^{12}\text{C}^{16}\text{O}_2)$. Taking the ratio of measured mole fractions of the two CO_2 isotopologues leads to the working equation

$$R(^{13}\text{C}/^{12}\text{C})_{\text{sample}} = \frac{a_r}{s_r}, \quad [1]$$

where the subscript r indicates the $(^{13}\text{C}^{16}\text{O}_2)/(^{12}\text{C}^{16}\text{O}_2)$ ratio of parameters, $a \equiv \int \alpha(\nu) d\nu$ are the measured peak areas for each line, and s_r is the line intensity ratio for the transition pair. By concurrent measurements of a for both $^{13}\text{C}^{16}\text{O}_2$ and $^{12}\text{C}^{16}\text{O}_2$ at similar signal-to-noise ratios, we also eliminated biases associated with the relative frequency axis as well as with the choice of line shape profile.

Substituting Eq. [1] into the definition $\delta^{13}\text{C} = R(^{13}\text{C}/^{12}\text{C})_{\text{sample}}/R(^{13}\text{C}/^{12}\text{C})_{\text{VPDB}} - 1$ and solving for $R(^{13}\text{C}/^{12}\text{C})_{\text{VPDB}}$ gives the VPDB reference value as

$$R(^{13}\text{C}/^{12}\text{C})_{\text{VPDB}} = \frac{a_r/s_r}{1+\delta^{13}\text{C}}, \quad [2]$$

where all quantities on the right-hand-side are based on values with quantifiable uncertainties.

We emphasize that the line intensities used to evaluate $R(^{13}\text{C}/^{12}\text{C})_{\text{sample}}$ in Eq. [1] depend upon invariant molecular constants and a temperature-dependent function describing Boltzmann population statistics (Supplementary Information, Section S3). As already stated, the temperature dependence of $s_r(T)$ was effectively eliminated by the choice of $^{13}\text{C}^{16}\text{O}_2$ and $^{12}\text{C}^{16}\text{O}_2$ transition pairs (Supplementary Information, Section S1). For $^{13}\text{C}^{16}\text{O}_2$, we used intensities calculated here from an updated, fully *ab initio* dipole moment surface (DMS) and a semi-empirical potential energy surface (PES). This choice was justified by benchmarking the underlying quantum-chemistry theory against accurate experiments (Supplementary Information, Section S2).

AIR-IS measurements of $R(^{13}\text{C}/^{12}\text{C})_{\text{sample}}$ for five CO_2 -in-air samples are plotted in Fig. 2A vs. $\delta^{13}\text{C}$ values assigned by IRMS (Supplementary Information, Section S4). In Fig. 2A, the fitted red dash-dotted line revealed a high degree of linearity between the two techniques ($r^2 = 0.997$), and fitted residuals are plotted in Fig. 2B. Note that the CO_2 -in-air samples were chosen to cover a broad range of $\delta^{13}\text{C}$ values that naturally occur across a wide variety of terrestrial and marine carbon sources, as illustrated in Fig. 2C. For example, AIR-IS $R(^{13}\text{C}/^{12}\text{C})_{\text{sample}}$ values are accurate enough to unambiguously differentiate between C3 and C4 plant photosynthetic pathways.

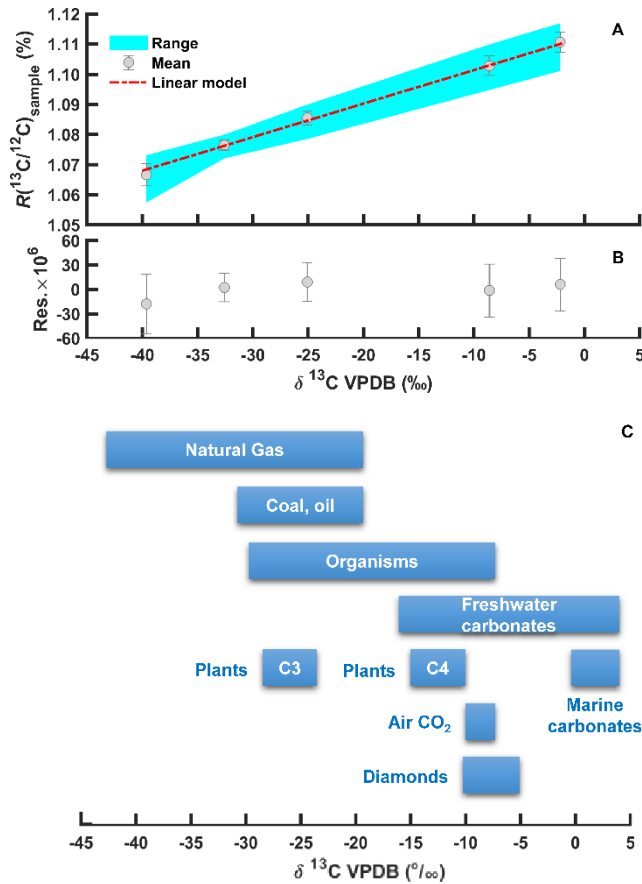


Fig. 2. AIR-IS measurements of $R(^{13}\text{C}/^{12}\text{C})_{\text{sample}}$ vs. IRMS assignments of $\delta^{13}\text{C}$. **A.** AIR-IS values of $R(^{13}\text{C}/^{12}\text{C})_{\text{sample}}$ were measured for five CO_2 -in-air samples with $\delta^{13}\text{C}$ VPDB value assignments by IRMS. The light-blue shaded region is the interpolated area bounded by the range of measured $R(^{13}\text{C}/^{12}\text{C})_{\text{sample}}$ values, while the mean and standard deviation for all five samples are plotted as gray circles. The red dash-dotted line represents a linear regression using the expression $R(^{13}\text{C}/^{12}\text{C})_{\text{sample}} = R(^{13}\text{C}/^{12}\text{C})_{\text{VPDB}} \times [(\delta^{13}\text{C}) + 1]$. **B.** Fitted residuals, along with their corresponding standard deviations. **C.** Example sources of terrestrial and marine carbon $\delta^{13}\text{C}$ values within the studied range.

With precise values of $\delta^{13}\text{C}$ assigned to our CO_2 -in-air samples traceability to VPDB, we used Eq. [2] to calculate $R(^{13}\text{C}/^{12}\text{C})_{\text{VPDB}}$ from each individual spectroscopic measurement of $R(^{13}\text{C}/^{12}\text{C})_{\text{sample}}$. A scatter plot of $R(^{13}\text{C}/^{12}\text{C})_{\text{VPDB}}$ versus an arbitrary measurement number is shown in Fig. 3A. From the ensemble statistics of $R(^{13}\text{C}/^{12}\text{C})_{\text{VPDB}}$ measured using samples with a variety of $\delta^{13}\text{C}$ values, we assessed long-term reproducibility associated with daily variations in the

spectrum signal-to-noise ratio. The scatter in the data points plotted in Fig. 3A included variability associated with spectroscopic interferences, as well as potential optical interference effects (e.g., spurious etalons) and daily variations in laser power and linewidth which slightly affected optical cavity throughput and scan speed. The data was fitted to a normal distribution function (Fig. 3B) with a mean value of $R(^{13}\text{C}/^{12}\text{C})_{\text{VPDB}} = 0.011125$ and a standard error of the mean of 1.7×10^{-6} . Therefore, our Type A evaluation of the long-term reproducibility gave a relative standard uncertainty of 0.15×10^{-3} .

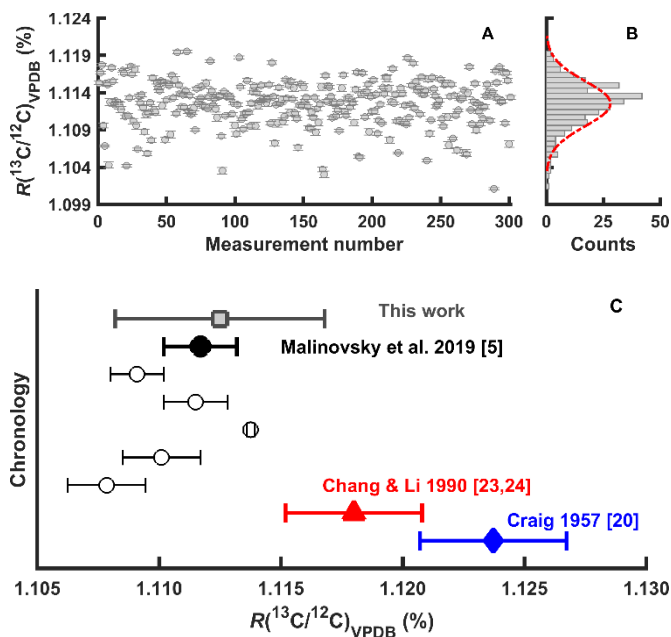


Fig. 3. AIR-IS value of $R(^{13}\text{C}/^{12}\text{C})_{\text{VPDB}}$. **A.** Scatter plot of all 301 unique AIR-IS measurements of $R(^{13}\text{C}/^{12}\text{C})_{\text{VPDB}}$, along with error bars showing relative precision of $\approx 0.2 \times 10^{-3}$. **B.** Histogram of values fitted to a normal distribution (red dash-dotted line), with mean value of $R(^{13}\text{C}/^{12}\text{C})_{\text{VPDB}} = 0.011125$. **C.** Comparison of literature values for $R(^{13}\text{C}/^{12}\text{C})_{\text{VPDB}}$ ^{5,20,23,24}, including this work. References for the black open circles are in Malinovsky et al.⁵ and the Supplementary Information. Error bars show combined standard uncertainty.

In addition to long-term reproducibility in a_r , we report persistent (systematic) relative standard uncertainties in $R(^{13}\text{C}/^{12}\text{C})_{\text{VPDB}}$ for the transition intensities, CRDS-signal digitizer

nonideality, choice of distribution function (Supplementary Information, Section S5), IRMS value assignments, and temperature in Table 1. Adding these components in quadrature gave a combined standard uncertainty in $R(^{13}\text{C}/^{12}\text{C})_{\text{VPDB}}$ of 43×10^{-6} .

Table 1. Summary of individual relative standard uncertainties (u) comprising the combined standard uncertainty for $R(^{13}\text{C}/^{12}\text{C})_{\text{VPDB}}$ of 43×10^{-6} reported in the main text.

Symbol	Value (10^{-3})	Notes
u_{636}	3.8	Line intensity, $^{13}\text{C}^{16}\text{O}_2$
u_{626}	0.6	Line intensity, $^{12}\text{C}^{16}\text{O}_2$
u_{ADC}	0.6	Digitizer nonideality
u_f	0.16	Choice of distribution function
u_{a_r}	0.15	Standard error in a_r
u_{IRMS}	0.06	IRMS $\delta^{13}\text{C}$ value assignments
u_T	0.04	Temperature-dependence of S

The value of $R(^{13}\text{C}/^{12}\text{C})_{\text{VPDB}}$ inferred from the unified AIR-IS and IRMS approach reported here is plotted as a gray square at the top of Fig. 3C and labeled “This work.” The error bar illustrates the combined standard uncertainty in our measurement, dominated by the uncertainty in the $^{13}\text{C}^{16}\text{O}_2$ transition intensities. For comparison, several literature values are also plotted in Fig. 3C. The blue diamond corresponds to the most widely cited value of $^{13}R_{\text{VPDB}} = 0.0112372$ (standard uncertainty, 30×10^{-6}), measured by calibrated mass spectrometry of the original PDB sample performed by Craig in 1957²⁰. More recently, in a 2010 technical report²³, the International Union of Pure and Applied Chemistry (IUPAC) recommended a value of $R(^{13}\text{C}/^{12}\text{C})_{\text{VPDB}} = 0.011180$ (standard uncertainty, 14×10^{-6}) based on mass spectrometry measurements by Chang & Li in 1990 (C&L, red triangle)²⁴. Additional experiments performed over the last 20 years (open black circles) collectively allude to an even lower absolute

value of $R(^{13}\text{C}/^{12}\text{C})_{\text{VPDB}} = 0.011117$ (standard uncertainty, 15×10^{-6}) show as the black dot⁵, with those literature values deviating by more than -14 ‰ from Craig²⁰.

The AIR-IS result is in good agreement with the 2019 recommendation of Malinovsky et al.⁵, suggesting from that a reevaluation of the internationally accepted value of $R(^{13}\text{C}/^{12}\text{C})_{\text{VPDB}}$ is appropriate. Recently, Skrzypek & Dunn²⁵ highlighted an immediate motivation for the adoption of an SI traceable, consensus value of $R(^{13}\text{C}/^{12}\text{C})_{\text{VPDB}}$. They report that three different reference values are currently in use by commercial optical stable carbon isotope analyzers, resulting in potential differences between calibrated analyzer δ values of $\approx 0.1 \text{ ‰}$. Therefore, the addition of our independent AIR-IS value to the VPDB discussion will aid in establishing consistency and traceability in stable carbon isotope analysis.

By directly interrogating highly homogenous gas-phase samples of CO_2 in air, AIR-IS avoids biases common to the general practice of CO_2 extraction from a VPDB traceable carbonate. Furthermore, AIR-IS also eliminates the need for O-isotope calibrations, potentially allowing the technique to accurately quantify $R(^{13}\text{C}/^{12}\text{C})_{\text{sample}}$ values even in the event of anomalous oxygen isotopic compositions. For example, careful attention must be paid to ^{17}O corrections when analyzing CO_2 samples with oxygen from different sources using mass spectrometry (e.g., samples originating from reactions with ^{17}O -enriched stratospheric ozone)²³. Oxygen isotope anomalies are also observed in extraterrestrial samples and may explain early solar system evolution²⁶. Specifically, the stable carbon isotopic composition of meteorites with potentially anomalous oxygen compositions reveal ^{13}C -enrichment in the organic molecules carried to early Earth²⁷. These O-isotope anomalies, unless known *a priori*, present a unique challenge for accurate mass spectrometry where oxygen corrections are explicitly required^{23,26}.

The accurate isotope ratio infrared spectroscopy methodology reported herein is suitable for the possible optical realization of various artifact-based scales, including ^{14}C , ^{18}O , ^{17}O , ^{15}N , ^2H , and ^{34}S . For stable carbon isotope ratios, our own efforts to ascertain more accurate values for $^{13}\text{C}^{16}\text{O}_2$ transition intensities in the 2 μm wavelength region using gravimetrically prepared, potentially isotopically enriched gas samples with traceability to the kilogram are just beginning. Accurate measurements of analogous $^{12}\text{C}^{16}\text{O}_2$ transitions could also reduce uncertainty in the $^{13}\text{C}^{16}\text{O}_2$ *ab initio* predictions (Supplementary Information, Section S2). Those results are expected to reduce our relative combined standard uncertainty associated $R(^{13}\text{C}/^{12}\text{C})_{\text{VPDB}}$ to $\leq 1 \times 10^{-3}$. Over time, a consensus optical determination of $R(^{13}\text{C}/^{12}\text{C})_{\text{VPDB}}$ through comparisons amongst national metrology institutes and their partners could ultimately obviate the current cumbersome and time-consuming task of artifact-based scale management and long-term scale propagation. Combined with recent advances in the optical detection of ^{14}C with sensitivity below the modern mole fraction of 1.176 pmol/mol^{28,29}, as well as emerging optical techniques for precision clumped isotope analysis³⁰, the possibility exists for finally realizing primary laser-based carbon and oxygen isotope metrology with traceability to the revised, “quantum” SI.

Acknowledgements

We acknowledge M. E. Kelley and W. R. Miller, Jr. (National Institute of Standards and Technology, NIST) for preparing several CO₂-in-air gas samples. Funding was provided by the NIST Greenhouse Gas and Climate Science Program. OLP acknowledges partial support from *Quantum Pascal* project 18SIB04, which received funding from the EMPIR programme co-financed by the

Participating States and the European Union's Horizon 2020 research and innovations programme. NFZ acknowledges State project 0035-2019-0016.

Author contributions

AJF assisted with experimental design, assembly, and characterization, performed data analysis, and wrote the letter. HY assembled optical instrumentation and performed spectroscopy on CO₂-in-air samples. AS performed isotope ratio mass spectrometry on parent CO₂ samples. OLP and NFZ performed quantum chemistry calculations of CO₂ transition intensities. JTH conceived the experimental design and assisted with instrumentation, data analysis, and reduction. All authors contributed to the final written letter.

Competing interests

The authors declare no competing financial interests.

References

1. Coplen, T. B. et al. New guidelines for $\delta^{13}\text{C}$ measurements. *Anal. Chem.* **78**, 2439-2441 (2006). [doi:10.1021/ac052027c](https://doi.org/10.1021/ac052027c)
2. Urey, H. C., Lowenstam, H. A., Epstein, S. & McKinney, C. R. Measurement of paleotemperatures and temperatures of the Upper Cretaceous of England, Denmark, and the Southeastern United States. *Geol. Soc. Am. Bull.* **62**, 399-416 (1951). [doi:10.1130/0016-7606\(1951\)62\[399:MOPATO\]2.0.CO;2](https://doi.org/10.1130/0016-7606(1951)62[399:MOPATO]2.0.CO;2)
3. Assonov, S. Summary and recommendations from the International Atomic Energy Agency Technical Meeting on the Development of Stable Isotope Reference Products (21-25 November 2016). *Rapid Commun. Mass Spectrom.* **32**, 827-830 (2018). [doi:10.1002/rcm.8102](https://doi.org/10.1002/rcm.8102)
4. Phillips, W. D. The end of artefacts. *Nature Phys.* **15**, 518 (2019). [doi:10.1038/s41567-019-0514-8](https://doi.org/10.1038/s41567-019-0514-8)
5. Malinovsky, D., Dunn, P. J. H., Holcombe, G., Cowen, S. & Goenaga-Infante, H. Development and characterization of new glycine certified reference materials for SI-traceable $^{13}\text{C}/^{12}\text{C}$

- isotope amount ratio measurements. *J. Anal. At. Spectrom.* **34**, 147-159 (2019).
[doi:10.1039/c8ja00281a](https://doi.org/10.1039/c8ja00281a)
6. Kerstel, E. "Isotope ratio infrared spectrometry" in Handbook of Stable Isotope Analytical Techniques, de Groot, P.A., Ed. (Elsevier, 2004), pp. 759–787. [doi:10.1016/B978-044451114-0/50036-3](https://doi.org/10.1016/B978-044451114-0/50036-3)
 7. Brand, W. A. & Coplen, T. B. Stable isotope deltas: tiny, yet robust signatures in nature. *Isotopes Environ. Health. Stud.* **48**, 393–409 (2012). [doi:10.1080/10256016.2012.666977](https://doi.org/10.1080/10256016.2012.666977)
 8. Brenna, J. T., Corso, T. N., Tobias, H. J. & Caimi, R. J. High-precision continuous-flow isotope ratio mass spectrometry. *Mass Spectrom. Rev.* **16**, 227–258 (1997). [doi:10.1002/\(SICI\)1098-2787\(1997\)16:5<227::AID-MAS1>3.0.CO;2-J](https://doi.org/10.1002/(SICI)1098-2787(1997)16:5<227::AID-MAS1>3.0.CO;2-J)
 9. Flores, E., Viallon, J., Moussay, P., Griffith, D. W. T. & Wielgosz R. I. Calibration strategies for FT-IR and other isotope ratio infrared spectrometer instruments for accurate $\delta^{13}\text{C}$ and $\delta^{18}\text{O}$ measurements of CO_2 in air. *Anal. Chem.* **89**, 3648-3655 (2017).
 10. Corso, T. N. & Brenna, J. T. High-precision position-specific isotope analysis. *Proc. Natl. Acad. Sci. U.S.A.* **94**, 1049–1053 (1997). [doi:10.1073/pnas.94.4.1049](https://doi.org/10.1073/pnas.94.4.1049)
 11. Webster, C. R. et al. Isotope ratios of H, C, and O in CO_2 and H_2O of the Martian atmosphere. *Science* **341**, 260-263 (2013). [doi:10.1126/science.1237961](https://doi.org/10.1126/science.1237961)
 12. Crosson, E. R. et al. Stable isotope ratios using cavity ring-down spectroscopy: determination of $^{13}\text{C}/^{12}\text{C}$ for carbon dioxide in human breath. *Anal. Chem.* **74**, 2003-2007 (2002). [doi:10.1021/ac025511d](https://doi.org/10.1021/ac025511d)
 13. Zare, R. N. et al. High-precision optical measurements of $^{13}\text{C}/^{12}\text{C}$ isotope ratios in organic compounds at natural abundance. *Proc. Natl. Acad. Sci. U.S.A.* **106**, 10928–10932 (2009). [doi:10.1073/pnas.0904230106](https://doi.org/10.1073/pnas.0904230106)
 14. Long, D. A., Okumura, M., Miller, C. E. & Hodges, J. T. Frequency-stabilized cavity ring-down spectroscopy measurements of carbon dioxide isotope ratios. *Appl. Phys. B* **105**, 471–477 (2011). [doi:10.1007/s00340-011-4518-z](https://doi.org/10.1007/s00340-011-4518-z)
 15. Castrillo, A. et al. Amount-ratio determinations of water isotopologues by dual-laser absorption spectroscopy. *Phys. Rev. A* **86**, 052515 (2012). [doi:10.1103/PhysRevA.86.052515](https://doi.org/10.1103/PhysRevA.86.052515)
 16. Kiseleva, M., Mandon, J., Persijn, S. & Harren, F. J. M. Line strength measurements and relative isotope ratio $^{13}\text{C}/^{12}\text{C}$ measurements in carbon dioxide using cavity ring down spectroscopy. *J. Quant. Spectrosc. Radiat. Transfer* **204**, 152–158 (2018). [doi:10.1016/j.jqsrt.2017.09.021](https://doi.org/10.1016/j.jqsrt.2017.09.021)
 17. Stoltmann, T., Casado, M., Daëron, M., Landais, A. & Kassi, S. Direct, precision measurements of isotopologue abundance ratios in CO_2 using molecular absorption

- spectroscopy: application to $\Delta^{17}\text{O}$. *Anal. Chem.* **89**, 10129-10132 (2017). [doi:10.1021/acs.analchem.7b02853](https://doi.org/10.1021/acs.analchem.7b02853)
18. Kääriäinen, T., Richmond, C. A. & Manninen, A. Determining biogenic content of biogas by measuring stable isotopologues $^{12}\text{CH}_4$, $^{13}\text{CH}_4$, and CH_3D with mid-infrared direct absorption laser spectrometer. *Sensors* **18**, 496 (2018). [doi:10.3390/s18020496](https://doi.org/10.3390/s18020496)
 19. Abe, M. et al. Dual wavelength 3.2- μm source for isotope ratio measurements of $^{13}\text{CH}_4/^{12}\text{CH}_4$. *Opt. Express* **23**, 21786-21797 (2015). [doi:10.1364/OE.23.021786](https://doi.org/10.1364/OE.23.021786)
 20. Craig, H. Isotopic standards for carbon and oxygen and correction factors for mass-spectrometric analysis of carbon dioxide. *Geochim. Cosmochim. Acta* **12**, 133–149 (1957). [doi:10.1016/0016-7037\(57\)90024-8](https://doi.org/10.1016/0016-7037(57)90024-8)
 21. Assonov, S., Groening, M., Fajgelj, A., Hélie, J.-F. & Hillaire-Marcel, C. Preparation and characterization of IAEA-603, a new primary reference material aimed at the VPDB scale realization for $\delta^{13}\text{C}$ and $\delta^{18}\text{O}$ determination. *Rapid Commun. Mass Spectrom.* **34**, e8867 (2020). <https://doi.org/10.1002/rcm.8867>
 22. 18th WMO/IAEA Meeting on Carbon Dioxide, Other Greenhouse Gases and Related Tracers Measurement Techniques (GGMT-2015), La Jolla, CA, USA, 13-17 September 2015, GAW Report No. 229. https://library.wmo.int/opac/doc_num.php?explnum_id=3074
 23. Brand, W. A., Assonov, S. S. & Coplen, T. B. Correction for the ^{17}O interference in $\delta(^{13}\text{C})$ measurements when analyzing CO_2 with stable isotope mass spectrometry (IUPAC Technical Report). *Pure Appl. Chem.* **82**, 1719–1733 (2010). [doi:10.1351/PAC-REP-09-01-05](https://doi.org/10.1351/PAC-REP-09-01-05)
 24. Chang, T. L. & Li, W.-J. A calibrated measurement of the atomic weight of carbon. *Chin. Sci. Bull.* **35**, 290–296 (1990). [doi:10.1360/sb1990-35-4-290](https://doi.org/10.1360/sb1990-35-4-290)
 25. Skrzypek, G. & Dunn, P. J. H. Absolute isotope ratios defining scales used in isotope ratio mass spectrometers and optical isotope instruments. *Rapid Commun. Mass Spectrom.* **34**, e8890 (2020). [doi:10.1002/rcm.8890](https://doi.org/10.1002/rcm.8890)
 26. Yurimoto, H. et al. “Origin and evolution of oxygen-isotopic compositions of the solar system” in *Protostars and Planets V*, Reipurth, B., Jewitt, D. & Keil, K., Eds. (The University of Arizona Press, 2007), pp. 849–862.
 27. Furukawa, Y. et al. Extraterrestrial ribose and other sugars in primitive meteorites. *Proc. Natl. Acad. Sci.* **116**, 24440-24445 (2019). [doi:10.1073/pnas.1907169116](https://doi.org/10.1073/pnas.1907169116)
 28. Galli, I. et al. Spectroscopic detection of radiocarbon dioxide at parts-per-quadrillion sensitivity. *Optica* **3**, 385–388 (2016). [doi:10.1364/OPTICA.3.000385](https://doi.org/10.1364/OPTICA.3.000385)

29. Fleisher, A. J., Long, D. A., Liu, Q., Gameson, L. & Hodges, J. T. Optical measurement of radiocarbon below unity fraction modern by linear absorption spectroscopy. *J. Phys. Chem. Lett.* **8**, 4550–4556 (2017). [doi:10.1021/acs.jpcllett.7b02105](https://doi.org/10.1021/acs.jpcllett.7b02105)
30. Prokhorov, I., Kluge, T. & Janssen, C. Optical clumped isotope thermometry of carbon dioxide. *Nat. Sci. Rep.* **9**, 4765 (2019). [doi:10.1038/s41598-019-40750-z](https://doi.org/10.1038/s41598-019-40750-z)

METHODS

Absolute isotope ratio infrared spectroscopy. We performed FARS CRDS³¹ using two DFB diode lasers simultaneously coupled to a single high-finesse enhancement cavity and sample cell. Long-term stability and reproducibility were achieved in part by actively stabilizing the uniform grid of optical frequencies transmitted by the enhancement cavity to a frequency-stabilized HeNe laser³². The enhancement cavity and sample cell comprised two triple-coated high-reflectivity mirrors at opposite ends of a stainless-steel tube. One of the mirrors was mounted to a piezo-electric transducer which was used as a slow actuator to adjust the cavity length to maintain resonance with the HeNe laser. The optical cavity was nominally 75 cm in length, with a free spectral range of 200.07 MHz (standard uncertainty, 30 kHz).

Before introduction of CO₂-in-air samples, the sample cell was evacuated under high vacuum for approximately 1 h and then flushed with a continuous flow of high-purity N₂ gas for approximately 2 h. The procedure effectively eliminated sample cell memory of the previous CO₂-in-air sample, as well as minimized spectroscopic interferences from previously adsorbed molecules within the gas delivery system. CO₂-in-air samples were then introduced and maintained at a constant pressure near 8 kPa (as measured by calibrated microbolometer gauges) for a total time of 2 h. After 2 h, the sample was evacuated, and the cavity prepared to receive another sample. Temperature stabilization was enhanced using an insulating box around the AIR-IS sample cell and was monitored during spectral acquisition using calibrated platinum resistance thermometers in good thermal contact with the outside of the enhancement cavity. A comprehensive summary of the NIST technical approach to accurate gas metrology by CRDS can be found in Fleurbaey et al.³³.

Digitizer linearity. Linearity of the analog-to-digital acquisition cards was tested using synthetic exponential decay signals (SEDS) and a metrology-grade reference digitizer as a transfer standard³⁴. The SEDS of 1 ms in length were constructed using an arbitrary waveform generator with 14-bit vertical resolution and a sampling rate of 128 MS/s. Their time constants spanned the relevant range for each digitizer; 26 μ s to 45 μ s for the 2.0 μ m digitizer (¹³C¹⁶O₂), and 10 μ s to 20 μ s for the 1.6 μ m digitizer (¹²C¹⁶O₂). Linear fits of observed SEDS time constants (τ_{obs}) vs. programmed time constants (τ_{pro}) yielded a transformation function between observed and true round-trip losses in the enhancement cavity. The linear transformations were used to estimate the relative shift in measured integrated absorption $\delta_a = \frac{a_{\text{obs}}}{a_{\text{pro}}} - 1$ for simulated lines at both 2.0 μ m and 1.6 μ m. The digitizer analysis yielded the following δ_a , which were then applied to all the measured spectra: $\delta_a = 4.7 \times 10^{-3}$ for ¹³C¹⁶O₂ at 2.0 μ m, and $\delta_a = -4.8 \times 10^{-3}$ for ¹²C¹⁶O₂ at 1.6 μ m. We estimated the uncertainty in δ_a to be equal to $\sqrt{2} \times 0.4 \times 10^{-3} \approx 0.6 \times 10^{-3}$ by fitting a generalized extreme value distribution function to the observed distribution in τ_{obs} over a broad range of SEDS. We note that the limit in the uncertainty in δ_a is calculated from the SEDS vertical resolution (14 bits) to be $1/(2^{\Delta+1}\sqrt{3}) \approx 0.02 \times 10^{-3}$. The measured values of δ_a estimated all potential non-linearities, impedance mismatches, radiofrequency back reflections, dissimilar metallic connectors, and other issues associated with all electronics and cable after the photoreceivers, including the digitizer.

Gas samples and $\delta^{13}\text{C}$ value assignments. Five CO₂-in-air samples were measured by AIR-IS. Mentioned in the main text is NIST Standard Reference Material (SRM[®]) 1720 Northern Continental Air with WMO/NOAA-assigned $\delta^{13}\text{C} = -8.6 \text{ ‰}$ (cylinder number CC324315 and sample number 1720-A-25)^{35,36}. The remaining four CO₂-in-air samples, having nominal CO₂ molar fractions approximately equal to atmospheric natural abundances ($\approx 400 \mu\text{mol/mol}$), were prepared at NIST. Briefly, the preparation

involved mixing (diluting) isotopically distinct pure CO₂ (>99.996 %) samples with a balance of synthetic air (N₂ = 78.1 %, O₂ = 20.89 %, CO₂ < 0.3 μmol/mol, N₂O < 0.2 nmol/mol) using gravimetric and volumetric standard preparation methods for compressed gas mixtures^{35,37}.

The VPDB-CO₂ δ¹³C and δ¹⁸O value assignments of these four samples were made at NIST on the parent CO₂ by dual inlet isotope ratio mass spectrometry (DI-IRMS)³⁸. The NIST VPDB-CO₂ scale realization was achieved using NIST pure CO₂ RMs 8562, 8563, and 8564³⁹. A summary of NIST DI-IRMS results and related gas sample information is available as Table S4 of the Supplementary Information. Importantly, the uncertainty of 0.06 ‰ associated with the NIST IRMS value assignments had a minimal impact on the absolute isotope ratio $R(^{13}\text{C}/^{12}\text{C})_{\text{VPDB}}$ estimated in this work. Further details regarding IRMS value assignment uncertainties can be found in Srivastava & Verkouteren³⁸ and in Section S4 of the Supplementary Information.

Isotope ratio notation and nomenclature. Here we use notation for isotope ratios recommended by the Commission on Isotopic Abundances and Atomic Weights of the International Union of Pure and Applied Chemistry (IUPAC)⁴⁰.

Quantum chemistry calculations. Rotational-vibrational transition intensities were calculated for ¹³C¹⁶O₂ using an updated *ab initio* dipole moment surface (DMS) and semi-empirical potential energy surface (PES). Here we improved upon the *ab initio* DMS of Polyansky et al.⁴¹ by increasing the number of *ab initio* data points by 50 % (3000 total points). Also, the semi-empirical PES of Huang et al.⁴², previously used by Polyansky et al.⁴¹ without modification, was fitted to known CO₂ energy levels using the DVR3D program⁴³ resulting in a standard deviation of 0.02 cm⁻¹. Analogous quantum chemistry methods recently applied to water (H₂O) showed that both an increased number of *ab initio* DMS data points⁴⁴ and an accurate semi-empirical PES⁴⁵ will improve accuracy in predicted transition intensities.

For our denser grid of *ab initio* points we applied the same level of quantum chemistry theory as Polyansky et al.⁴¹: an all-electron multireference configuration interaction (MRCI) calculation with the aug-cc-pwCVQZ basis set, inclusive of relativistic corrections determined from separately fitted one-electron mass-velocity-Darwin (MVD1) terms. Calculations used the MOLPRO package⁴⁶, and the wave functions—required to predict the transition intensities—were solved numerically from the rotational-vibrational Schrödinger equation using the DVR3D program⁴³.

To evaluate uncertainty in the predicted ¹³C¹⁶O₂ transition intensities, we also calculated transition intensities for ¹²C¹⁶O₂ and compared with highly accurate experiments^{33,47-49}. For ground-state rotational quantum numbers of $J'' = 12$ and $J'' = 18$ we find that, for five near-infrared vibrational bands of ¹²C¹⁶O₂, the standard deviation of a uniform distribution chosen to represent the experimental measurements relative to the predictions of our updated *ab initio* DMS is equal to 3.8×10^{-3} . This value, listed in Table 1 of the main text as the uncertainty in the ¹³C¹⁶O₂ transition intensities, is consistent with upper-bound estimates from quantum chemistry methods^{41,50}. Further details, including numerical results from the updated *ab initio* DMS and their comparison with the experimental literature, can be found in Sections S1 and S2 of the Supplementary Information.

References

31. Truong, G. W. et al. Frequency-agile, rapid scanning spectroscopy. *Nat. Photon.* **7**, 532-534 (2013). [doi:10.1038/nphoton.2013.98](https://doi.org/10.1038/nphoton.2013.98)
32. Hodges, J. T., Layer, H. P., Miller, W. W. & Scace, G. Frequency-stabilized single-mode cavity ring-down apparatus for high-resolution absorption spectroscopy. *Rev. Sci. Instrum.* **75**, 849-863 (2004). [doi:10.1063/1.1666984](https://doi.org/10.1063/1.1666984)

33. Fleurbaey, H., Yi, H., Adkins, E. M., Fleisher, A. J. & Hodges, J. T. Cavity ring-down spectroscopy of CO₂ near $\lambda = 2.06 \mu\text{m}$: Accurate transition intensities for the Orbiting Carbon Observatory-2 (OCO-2) “strong band.” *J. Quant. Spectrosc. Radiat. Transfer* **252**, 107104 (2020). [doi:10.1016/j.jqsrt.2020.107104](https://doi.org/10.1016/j.jqsrt.2020.107104)
34. Fleisher, A. J. et al. Twenty-five-fold reduction in measurement uncertainty for a molecular line intensity. *Phys. Rev. Lett.* **123**, 043001 (2019). [doi:10.1103/PhysRevLett.123.043001](https://doi.org/10.1103/PhysRevLett.123.043001)
35. Rhoderick, G. C. et al. Development of a Northern Continental Air Standard Reference Material. *Anal. Chem.* **88**, 3376-3385 (2016). [doi:10.1021/acs.analchem.6b00123](https://doi.org/10.1021/acs.analchem.6b00123)
36. NOAA Central Calibration Laboratory reference gas calibration results for NIST Standard Reference Material 1720 Northern Continental Air serial number CC324315 available at <https://www.esrl.noaa.gov/gmd/ccl/refgas.html>.
37. Milton, M. J. T., Guenther, F., Miller, W. R. & Brown, A. S. Validation of gravimetric values and uncertainties of independently prepared primary standard gas mixtures. *Metrologia* **43**, L7-L10 (2006). [doi:10.1088/0026-1394/43/3/N01](https://doi.org/10.1088/0026-1394/43/3/N01)
38. Srivastava, A. & Verkouteren, R. M. Metrology for stable isotope reference materials: ¹³C/¹²C and ¹⁸O/¹⁶O isotope ratio value assignment of pure carbon dioxide gas samples on the Vienna PeeDee Belemnite-CO₂ scale using dual-inlet mass spectrometry. *Anal. Bioanal. Chem.* **410**, 4153-4163 (2018). [doi:10.1007/s00216-018-1064-0](https://doi.org/10.1007/s00216-018-1064-0)
39. Verkouteren, R. M. & Klinedinst, D. B. Value assignment and uncertainty estimation of selected light stable isotope reference materials: RMs 8543-8545, RMs 8562-8564, and RM 8566. NIST Special Publication 260-149 (2004). <https://www.nist.gov/document-10350>
40. Coplen, T. B. Guidelines and recommended terms for expression of stable-isotope-ratio and gas-ratio measurements results. *Rapid Commun. Mass Spectrom.* **25**, 2538-2560 (2011). [doi:10.1002/rcm.5129](https://doi.org/10.1002/rcm.5129)
41. Polyansky, O. L. et al. High-accuracy CO₂ line intensities determined from theory and experiment. *Phys. Rev. Lett.* **114**, 243001 (2015). [doi:10.1103/PhysRevLett.114.243001](https://doi.org/10.1103/PhysRevLett.114.243001)
42. Huang, X., Schwenke, D. W., Tashkun, S. A. & Lee, T. J. An isotopic-independent highly accurate potential energy surface for CO₂ isotopologues and an initial ¹²C¹⁶O₂ infrared line list. *J. Chem. Phys.* **136**, 124311 (2012). [doi:10.1063/1.3697540](https://doi.org/10.1063/1.3697540)
43. Tennyson, J. et al. DVR3D: a program suite for the calculation of rotation-vibration spectra of triatomic molecules. *Comput. Phys. Commun.* **163**, 85 (2004). [doi:10.1016/j.cpc.2003.10.003](https://doi.org/10.1016/j.cpc.2003.10.003)
44. Conway, E. K., Kyuberis, A. A., Polyansky, O. L., Tennyson, J. & Zobov, N. F. A highly accurate *ab initio* dipole moment surface for the ground electronic state of water vapour for spectra extending into the ultraviolet. *J. Chem. Phys.* **149**, 084307 (2018). [doi:10.1063/1.5043545](https://doi.org/10.1063/1.5043545)
45. Mizus, I. I. et al. High-accuracy water potential energy surface for the calculation of infrared spectra. *Phil. Trans. R. Soc.* **376**, 20170149. [doi:10.1098/rsta.2017.0149](https://doi.org/10.1098/rsta.2017.0149)
46. Werner, H.-J., Knowles, P. J., Knizia, G., Manby, F. R. & Schütz, M. Molpro: a general-purpose quantum chemistry program package. *Wiley Interdiscip. Rev.: Comput. Mol. Sci.* **2**, 242 (2012). [doi:10.1002/wcms.82](https://doi.org/10.1002/wcms.82)
47. Long, D.A. et al. High-accuracy near-infrared carbon dioxide intensity measurements to support remote sensing. *Geophys. Res. Lett.* **47**, e2019GL086344. [doi:10.1029/2019GL086344](https://doi.org/10.1029/2019GL086344)
48. Wübbeler, G., Viquez, G. J. P., Jousten, K., Werhahn, O. & Elster, C. Comparison and assessment of procedures for calculating the R(12) line strength of the $\nu_1 + 2\nu_2 + \nu_3$ band of CO₂. *J. Chem. Phys.* **135**, 204304 (2011). [doi:10.1063/1.3662134](https://doi.org/10.1063/1.3662134)

49. Yi, H., Liu, Q., Gameson, L., Fleisher, A. J. & Hodges, J. T. High-accuracy $^{12}\text{C}^{16}\text{O}_2$ line intensities in the $2\ \mu\text{m}$ wavelength region measured by frequency-stabilized cavity ring-down spectroscopy. *J. Quant. Spectrosc. Radiat. Transfer* **206**, 367-377 (2018).
50. Lodi, L. & Tennyson, J. Line lists for H_2^{18}O and H_2^{17}O based on empirical line positions and *ab initio* intensities. *J. Quant. Spectrosc. Radiat. Transfer* **113**, 850-858 (2012).
[doi:10.1016/j.jqsrt.2012.02.023](https://doi.org/10.1016/j.jqsrt.2012.02.023)